Original Article

Two-tiered reconstruction of Late Pleistocene to Holocene changes in the freezing level height in the largest glacierized areas of the Colombian Andes

Daniel RUIZ-CARRASCAL[1]* (iD) https://orcid.org/0000-0003-0987-5017; e-mail: pfcarlos@iri.columbia.edu

Daniel GONZÁLEZ-DUQUE[2] (iD) https://orcid.org/0000-0001-8328-283X; e-mail: daniel.gonzalez@vanderbilt.edu

Isabel RESTREPO-CORREA[3] (iD) https://orcid.org/0000-0002-1338-159X; e-mail: irestrco@eafit.edu.co

*Corresponding author

1 Department of Ecology, Evolution and Environmental Biology, Columbia University in the City of New York, New York, NY 10027, USA

2 Department of Civil and Environmental Engineering, Vanderbilt University, 400 24th Avenue South, 269 Jacobs Hall, Nashville TN 3720, USA

3 Department of Earth Sciences, Universidad EAFIT, Carrera 49 No. 7Sur-50, Medellín, Colombia

Abstract: One way of deducing vertical shifts in the altitudinal distribution of Colombian high-altitude páramo environments is by inferring fluctuations in the height of the local freezing level. In our research, we are implementing two complementary approaches to reconstruct Late Pleistocene to Holocene changes in the freezing level height (FLH) in two of the most extensively glacier-covered areas of the northern Andes. We combined remote sensing and field-based geomorphological mapping with time-series reconstruction of changes in the altitude of the 0°C isotherm. Changes in the FLH were based on already-published ~30 kyr paleo-reconstructions of sea surface temperatures (SSTs) of the eastern tropical Pacific and the western tropical Atlantic, as well as on reconstructed long-term sea level changes and empirical orthogonal functions of present-day (historical) Indo-Pacific and tropical Atlantic SST anomalies. We also analyzed the probability distribution of air-sea temperature differences and the spatial distribution of grid points with SSTs above the minimum threshold necessary to initiate deep convection. We considered available historical near-surface and free air temperature data of ERA-Interim reanalysis products, General Circulation Model (GCM) simulations, weather stations, and (deployed by our group) digital sensors, to assess the normal Environmental Lapse Rates (ELRs) at the regional to local scale. The combined maps of glacial landforms and our reconstructed FLHs provided us with a well-founded inference of potential past glacier advances, narrowing down the coarse resolution of ice margins suggested by previous research efforts. The extent of the areas with temperatures below the freezing point suggested here for the summits of our main study site exceeds in magnitude the corresponding glacier ice-caps and front advances proposed by previous studies. Conversely, our average lowest altitudes of the FLH for our comparative site are consistently above the main glacier-front advances previously suggested. Our results indicate that, compared to the maximum upward changes that likely took place over the past ca. 20,000 years in our two areas of interest, the

observed (present-day) upward shifts of the FLH have occurred at a rate that significantly surpasses our inferred rates. Our study helps fill the gaps in understanding past climatic changes and present trends in the region of interest and provides some insights into analyzing the signals of natural and anthropogenic climate change.

Keywords: Glacial events; Colombian Andes; Climate reconstruction; Geomorphology; Mountain glaciers; Freezing level height

1 Introduction

The upper ranges of the northern Andes consist of a mosaic of humid montane forests, tundra-like páramo ecosystems, isolated snowfields, and mountain glaciers. These unique, highly diverse neotropical high-altitude environments are currently experiencing unprecedented climatic changes (Vuille and Bradley 2000; Bradley et al. 2004; Bradley et al. 2006; Vuille et al. 2008; Bradley et al. 2009; Rabatel et al. 2013; Schauwecker et al. 2014; Vuille et al. 2015). As in the case of many mountain environments on the planet but not everywhere (Pepin et al. 2015; Wang et al. 2016; Qixiang et al. 2018), the upper levels of the northern Andes are facing increases in near-surface air temperatures that are occurring faster than in their surrounding low-elevation counterparts. Understanding how high-altitude Andean environments were distributed under past environmental conditions and how they responded to past climatic changes could provide us with insights into how they might respond to the ongoing fast climatic forcing.

Reconstructions of past climatic conditions in the Andes have been of interest to many research groups. A recent review paper (Palacios et al. 2020) synthesizes the full list of articles on the evolution of glaciation in the Americas during the Last Glacial Termination, and devotes a portion of the paper to long-term changes in climatic conditions in the tropical Andes. In terms of the paleoecological history of the high Andes, there is also a long list of efforts. In the studies by Thompson et al. (1984, 1985, 1986, 1988, 1995, 1998, 2000), which are based on stratigraphy and analysis of dust layers, nitrate and pollen concentrations, and assessments of oxygen isotopes in ice-cores from mountain peaks in the high central Andes, the authors suggest that fluctuations in

environmental conditions and major climate drivers such as El Niño-Southern Oscillation (ENSO) events have a profound influence on Andean high-altitude environments. Research by Bush et al. (1990) and Clapperton (1993), revisited by Thompson et al. (2000), which were based on ice-core and pollen palaeoclimatic records, have pointed to inferred shifts in major vegetation types from the Last Glacial Maximum (ca. 20 kyr) to present-day, and have provided a continental-wide distribution of Andean glaciers, ice caps, and montane grasslands. Specifically for the páramos, the palaeoecological history of these environments over the Pliocene and the entire length of the Pleistocene has been of interest to many researchers (van der Hammen 1974; Cleef 1979; Hooghiemstra 1984; Hooghiemstra and van der Hammen 2004) and has prompted studies such as the one by Flantua et al. (2019) who used a previously collected (Torres et al. 2013) high-resolution fossil pollen record to quantify the effects of climate fluctuations of the last 1 Myr on the páramos connectivity.

The geological and ecological approaches mentioned above used a wide variety of techniques to assess fluctuations between cold and warm stages. As stated, their techniques ranged from the analysis of glacial landforms, particularly moraines, erratic boulders and polished bedrock, to detailed pollen counts. The former can be used to directly determine changes in precipitation and temperature during cold stades, whereas the latter could lead to the assessment of changes during mild and warm periods. These approaches also focused on different lengths and timescales of the past periods to be reconstructed, ranging from millions to thousands of years. In order to build the extensive and exhaustive assessment of the potential effects of climate fluctuations on the extent of mountain habitats in the northern Andes, these studies demanded considerable resources for running field campaigns and laboratory assays. In our limited-funding research initiative, which is still in its early stages, we propose a freely accessible online satellite and climate data-driven approach to understand how fast climatic changes have occurred in the upper ranges of the northern Andes. Our proposal is not intended to compete with or argue against the multiple glaciological and paleoecological research efforts conducted in the Andes. Instead, our study aims to complement the vast list of research efforts mentioned above. Our short-term goal is to

infer how high-altitude páramo environments have been colonizing their harsh environments under the dissimilar signals of natural and anthropogenic climate change.

One way of deducing vertical shifts in the altitudinal distribution of the páramos is by inferring fluctuations in the height of the local freezing level, as páramos maintain over long time intervals their relationship to the snowline, acknowledging that neither the snowline nor the glacial margins automatically represent the 0°C-isotherm. Research on the spatio-temporal variability of the altitude of the 0°C isotherm or freezing level height (FLH) in the Andes has been explored by various teams, including Schauwecker et al. (2017), who argued that the FLH during precipitation events (Francou et al. 2004) and the snowfall level height or snow/rain transition height are closely related. The approach of using the FLH to infer the snowline comes, of course, with multiple challenges, caveats, and uncertainties. Although glaciations in low-latitude Alpine environments preserve one of the best records of past climatic conditions (Kaser and Georges 1999), in-depth glaciological studies in low latitudes are still scarce. In addition, unlike the slow ebb and flow of continental ice sheets in high latitudes, mountain glaciers in the northern equatorial Andes respond very rapidly to climatic changes (Kaser 2001; Kaser and Osmaston 2002). Even in extensively glacier-covered massifs, equatorial glaciers tend to be small (Vuille et al. 2018) because of the fast build-up of their ice caps. Except in the highest summits of the tropical Andes (>6,000 m), glaciers near the Equator usually have thin valley outlet tongues constantly close to melting. When their thin glacier tongues recede, they leave behind barely noticeable unconsolidated glacial debris, making the identification of past glacial advances a significant challenge.

Colombia has many of those small glaciers, all of them located on top of the highest summits of three mountainous areas, namely the Sierra Nevada de Santa Marta on the Caribbean coast and the Eastern and Central cordilleras, both in the Andean region (Fig. 1-A). At the beginning of the industrial era, the total extent of mountain glaciers in Colombia was about 349 km² (IDEAM 2018). The total present-day extent reaches only 37 km², and the average lower altitude of ice caps margins is at 4,800 m. The largest glacierized extent in Colombia used to be on the Ruiz-Tolima volcanic massif in the Central cordillera. In fact, it was once considered 'one of the most extensively glacier-covered massifs in the northern Andes' (Herd 1974; Thouret 1988). The Ruiz-Tolima has been of interest to previous research efforts (Herd 1982; Salomons 1986; van der Hammen 1989; Flórez 1992a; Flórez 1992b; Thouret et al. 1996; Velásquez 1998; Braitmeyer 2003; Bromley et al. 2013; and the compilation of López-Arenas and Ramírez-Cadena 2010). The paleoecological history of the last 50 to 6 kyr has been reconstructed through volcanic soil sequences, glacial geomorphology, mineralogy, sediments, and pollen deposits (Kuhry et al. 1983; Bakker and Salomons 1989; Cleef et al. 1995; Thouret et al. 1997). In particular, Thouret et al. (1996 and references therein) suggested several cold stades for the volcanic massif during the Upper Pleistocene, encompassing from the Early Río Recio stade (>48 kyr) and the Early to Middle full glacial (28-21 kyr) to the Early Neoglacial (~0.6 kyr). Even though this information has very broad age assignations and low resolution, it is the only available glacial record for the Ruiz-Tolima volcanic complex.

Correlations were established to link this set of cold stades with those previously reported by van der Hammen et al. (1995). These inferences were later combined with the geologic mapping of some mountain glaciers in the Eastern cordillera to propose a Quaternary glacier record for the Colombian Andes (Helmens 2004). All these publications agreed on the timing of cold stades and suggested that the main trigger that controls climatic conditions in the upper ranges of the Colombian Andes is the temporal dynamics of the Atlantic Ocean. Recent projects have proposed that there might be differences between the main factors driving local and regional conditions in the three Colombian cordilleras. Based on palynological and X-ray fluorescence analyses of sediment cores sampled in a study site in the Páramo de Frontino on the Colombian Western cordillera, Muñoz et al. (2017) concluded that local climatic conditions in the Western cordillera are driven by the main modes of variability of Pacific sea surface temperatures. In other words, local climatic conditions are dominated by ENSO dynamics. Therefore, there is still a need to deepen our understanding of the main drivers behind the occurrence of cold stades in a region that gets the combined signals of the Atlantic and the Pacific oceans, i.e., in the Central cordillera.
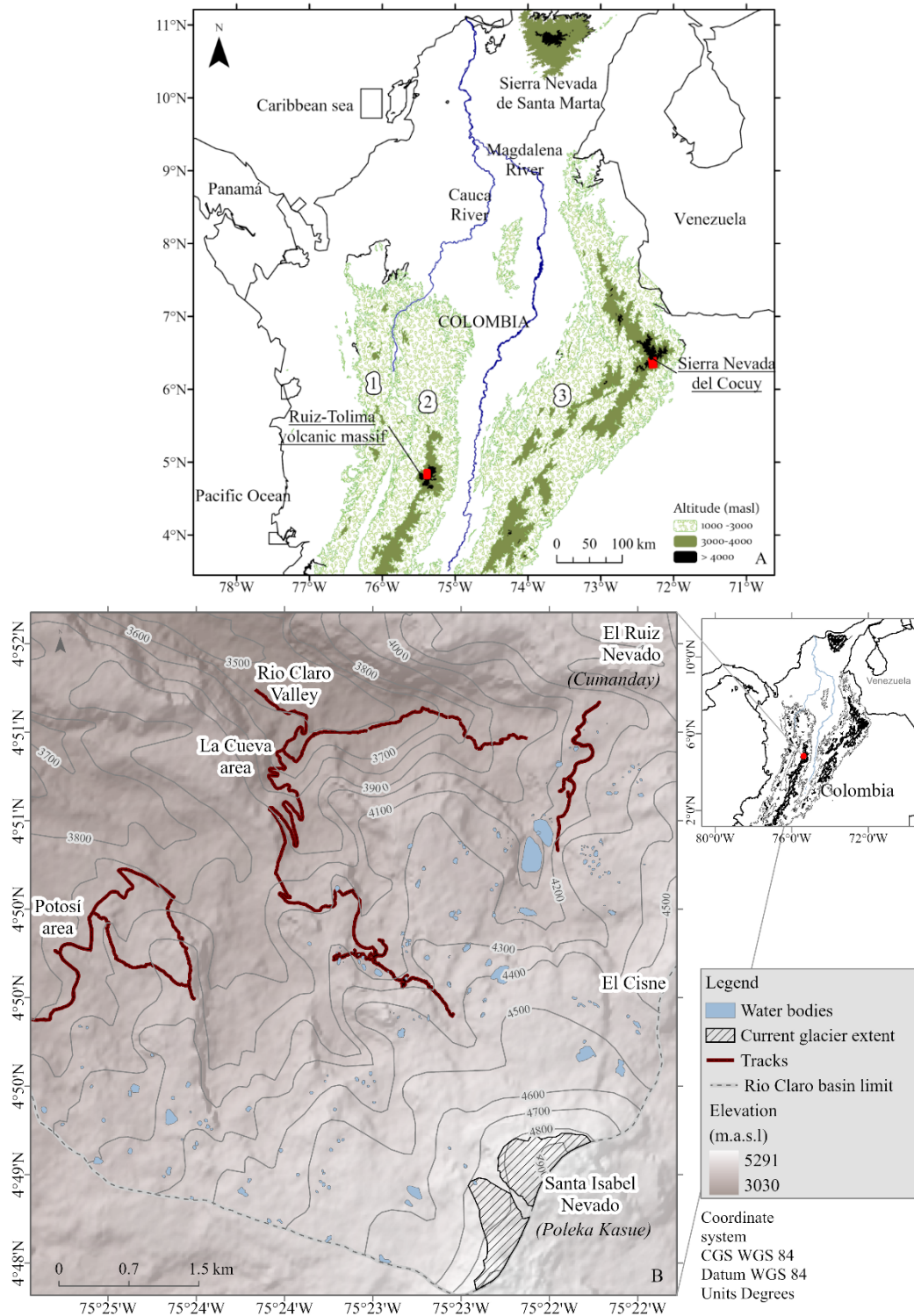
Fig. 1 Study sites. (A) General location of the two study sites in the Colombian territory (see red dots). The western, central and eastern cordilleras of the Colombian Andes are labeled (1), (2) and (3), respectively. Black solid areas depict elevational ranges higher than 4,000 m above present-day sea level. The main research site –the Ruiz-Tolima volcanic massif– is on the central cordillera, whereas the comparative study site –the Sierra Nevada del Cocuy site– is located on the eastern cordillera. For reference, the Sierra Nevada de Santa Marta on the Caribbean coast is also shown. (B) Tracks and trails taken to map geomorphological features in the headwaters of the Claro river high-altitude basin and reach potential confounders and misinterpretations. The dashed line depicts the watershed boundary. Striped area represents the present-day glacier extent on the Santa Isabel nevado.

In our research, we are merging two complementary approaches to reconstruct Late Pleistocene (c. 129 to c. 11.7 kyr) to Holocene (c. 11.7 kyr to present) changes in the freezing level height in two of the most extensively glacier-covered areas in the northern Andes. Our study areas are located in the northernmost region (the so-called *inner tropics* region) of the seven distinct climatic groups in the Andes (Sagredo and Lowell 2012). The inner tropics are characterized by the following important aspects: (i) high precipitation amounts are the norm. (ii) The Equilibrium Line Altitude – ELA (or the altitude on a glacier at which the total annual ablation equals the total annual accumulation) is more sensitive to changes in temperature than to changes in precipitation, and its sensitivity is greatest compared to other regions along the Andes. (iii) ELA responds linearly to changes in temperature, and the magnitude of such a response is determined by local environmental lapse rates (Sagredo et al. 2014). (iv) The response of humid glaciers in this region to changes in climatic conditions tends to happen very fast (i.e., they exhibit little lag time; Kaser et al. 2003). (v) The present-day ELA is located at altitudes slightly below 5 km (Sagredo et al. 2014), and thus it is influenced by temperatures in the upper tropical troposphere. (vi) The elevation of the 0°C atmospheric isotherm exhibits a small annual range (Klein et al. 1999), promoting melting of the lower parts of mountain glaciers all year round. And, (vii) glacier snowlines can be found several hundred meters below the 0°C isotherm, as documented by Klein et al. (1999) for modern glacier snowlines (elevations from 4,400-4,700 m) in the wet eastern tropical Andes. Our interest is to identify long-term changes in climatic and environmental conditions based on two approaches: geomorphological mapping of glacial landforms, and time-series reconstruction of changes in the altitude of the 0°C isotherm, both at the local scale. Improved knowledge of these changes and the main drivers behind glacial retreat is becoming a critical priority, given our need to assess the past, present, and future extent of high-altitude páramo environments in the upper ranges of the northern Andes.

2 Study Area

Our main study site is located on the northwestern flank of the Ruiz-Tolima volcanic massif, more specifically in the Claro river high-altitude basin, whose headwaters lie within a key protected area known locally as Los Nevados Natural Park, which is confined to the upper ranges of the vast volcanic complex. The full spatial domain of interest extends from 04°30'N to 05°00'N, and from 75°10'W to 75°40'W, and covers a portion of the Colombian Central cordillera and its two adjacent inter-Andean valleys (Fig. 1-A). In the volcanic complex, the loss of ice caps has been noted since the mid- to late-1800s. Three small glaciers, namely Quindío, Santa Rosa, and El Cisne, fully disappeared during the 20th century (Williams Jr. and Ferrigno 1999). Currently, only three volcanos still have ice-caps. They are the El Ruiz (or *Cumanday* in the local indigenous language; 5,321 m), the Santa Isabel (*Poleka Kasue*; 5,100 m), and the Tolima (*Dulima*; 5,280 m) nevados. Their current glacierized areas are of about 8.4, 0.63, and 0.58 km², and the lowest altitude of their ice-margins reaches 4,800 m, 4,700 m, and 4,900 m, respectively.

The Claro river basin, to approximately 1,800 m where the Claro watercourse meets the Los Molinos River, has a drainage area of about 191 km². Its main stream is fed by numerous creeks whose headwaters cover large areas of the snowfields and ice caps of the soon-to-disappear Ruiz and Santa Isabel ice-capped volcanoes (Fig. 1-B). In the mid-1980s, the lowest average altitudinal limit of their glacier margins was 4,700 m, forming ice caps of about 21 and 10 km² on the summits of these two nevados. In the mid-1990s, the average ELA in the Ruiz-Tolima volcanic massif was located 400 m above the 1980s ice margins, close to the corresponding mean annual 0°C isotherm (Thouret et al. 1996). This ELA was unevenly located on both slopes of the volcanic complex (it was a few tens of meters lower on the eastern side; Herd 1974) due to the rain-shadow effect on the west flank of the massif and due to the higher environmental lapse rate on the eastern flank. The present-day mean annual freezing point height is probably slightly above 5,100 m, consistent but higher than the average FLH suggested for the 20°S to 20°N tropical regions, which ranges from 4,500 to 5,000 m (Harris et al. 2000). Since the Arenas caldera of the Ruiz nevado has been active, producing multiple convecting plumes of ash in its recent history, most of the unconsolidated glacial debris on the massif are buried under a thick layer of pyroclastic debris and tephra deposits. Only the very recent history (~500 years) of moraine units

are well preserved and not mantled under such layers (Bromley et al. 2013). All these characteristics add complexity to our research on past glacial advances and retreats in the area.

There is only one weather station located at high altitude in the Los Nevados with a long instrumental period (1981 to present): Las Brisas, 04°56'N, 75°21'W, 4,150 m. Based on the available records, near-surface minimum temperatures exhibit a bi-modal annual cycle which is above the freezing point but below +3°C, with peaks commonly occurring in the months of May-June and October-November, and periods of low values usually taking place in the months of December-January and July-August. Liquid precipitation shows an annual cycle with two peaks, commonly occurring in the quarters Mar-April-May and September-October-November, whose monthly values range from 100 to 200 mm. Dry seasons are observed during the quarters December-January-February and June-July-August, with monthly rainfall amounts in the range 50-100 mm. There are no records of solid precipitation.

Our inferences for the main study site are compared with glacial advances of the Pan de Azúcar (5,100 m) and Campanillas Blanco (4,900 m) nevados and the already-vanished Campanillas Negro (4,800 m) along the headwaters of the Lagunillas river basin, which is located on the southwestern flank of the Sierra Nevada del Cocuy, in the Eastern cordillera. This comparative site is also located within a protected area, known as the Sierra Nevada del Cocuy (Chita or Güicán) national park. The full spatial domain of interest extends from 06°19'N to 06°26'N, and from 72°17'W to 72°23'W (Fig. 1-A). The protected area hosts the largest glacierized area of Colombia nowadays. Its present-day glacier extent reaches 13.3 km² (IDEAM 2018), which is distributed among 21 mountain peaks. The local largest ice-capped area (ca. 4.4 km²) is located on top of the Ritak'Uwa Blanco (5,380 m), and the lowest altitude of its ice-margins reaches 4,700 m.

The Lagunillas basin, to approximately 3,300 m where its main stream meets the Cóncavo river, has a drainage area of about 31 km². It is fed by the Bocatoma/Agua Bendita Creek, whose headwaters get the inflow of melting ice caps from the Pan de Azúcar and Campanillas Blanco nevados, and the ephemeral snowfields of the Campanillas Negro peak. It is worth mentioning that this study site is located 12 km to the south of the Ritacuba Negro river basin, which is also located on the western flank of the Sierra Nevada, and that was the focus of the research by Jomelli et al. (2014). The present-day (2003) frontal position of the glacier in the Ritacuba Negro basin reported in their article was located at 4,660 m above sea level. There are no weather stations with long instrumental periods located at high altitude in this area.

3 Data

3.1 Satellite and digital elevation model data

We processed free 2017 three-color band Bing satellite images available at a 2.68E-06° spatial resolution, which is roughly equivalent to a 0.30-m grid spatial scale. The Bing geographic domain for Los Nevados extends from 75°25'W to 75°20'W and from 04°48'N to 04°53'N, approximately. In the Sierra Nevada del Cocuy, the geographic domain extends from 72°23'W to 72°17'W and from 06°20'N to 06°26'N, approximately. Aerial photographs covering the full extent of the main study area (Los Nevados) are not available because scarce flight paths have crossed far south and east to the area of interest. For the full extent of the tropical Andes, we processed the quality-controlled NOAA NGDC GLOBE gridded 1-km global Digital Elevation Model (Hastings and Dunbar 1999).

3.2 Paleo data

We processed recent paleo-reconstructions of eastern tropical Pacific sea surface temperatures (SSTs) published by Kienast et al. (2006), Bova et al. (2015), and Dyez et al. (2016), as well as paleo-reconstructions of sea level changes proposed by Lea et al. (2000, 2002) and Waelbroeck et al. (2002). Sea level reconstructions are important because sea level itself could cause an apparent rise/fall in the FLH, regardless of actual climate variability. We also explored three additional paleo time series to complement our analyses and estimates: the temperature difference (from the present) from the Vostok ice core (Jouzel et al. 1987; Petit et al. 1990); the $^{18}O/^{16}O$ isotopic ratio from the Greenland Ice-core Project – GRIP (Dansgaard et al. 1993; GRIP members 1993); and the ~25 kyr to present paleo-reconstruction of western tropical Atlantic SSTs, published by Lea et al. (2003). The paleo-

reconstructed SSTs used here were selected among the various locations of SST proxy data sites (Shakun et al. 2012; Marcott et al. 2013).

3.3 Historical sea surface temperature data

We processed monthly sea surface temperature anomalies (SSTa) available for the [30°S-30°N, 30°E-90°W] and [30°S-30°N, 60°W-15°E] spatial domains of the tropical Indo-Pacific and the tropical Atlantic oceans, respectively (Kaplan et al. 1998). These reconstructed and observed SSTa data comprise the period spanning from January 1856 to December 2017 and are available at a 5°-arc spatial resolution. Analyses were complemented with the improved and extended, reconstructed global NOAA NCDC ERSST version2 SST data (based on COADS data; Smith and Reynolds 2004), which span the period January 1854 - December 2009. Present-day SSTs observed in the Niño 1+2 and Niño 3.4 regions of the eastern and central Tropical Pacific were also analyzed. These data are available for the historical period spanning from January 1950 to December 2017. Lastly, we complemented our analyses with the 1°-arc fields of monthly SST (0.0 depth) from the LEVITUS94 - World Ocean Atlas 1994 (Levitus and Boyer 1994).

3.4 Reanalysis and GCM air temperature data

We processed climatological monthly mean air temperatures at 2 meters above ocean surface from NOAA NCEP/DOE AMIP-II Reanalysis (hereafter called Reanalysis-2; Kanamitsu et al. 2002) for the historical period 1980-2009. Near-surface air temperatures in the spatial domain [30°S-30°N, 30°E-90°W] and the narrower domain [12.5°S-12.5°N, 187.5°E-90°W] were of interest. We also processed mean monthly near-surface and free air temperature Reanalysis-2 data for a set of grid points located along the main axis of the Andes cordillera. These data are available for the historical period spanning from January 1979 to June 2014. We analyzed the North American Regional Reanalysis 3-hr temperature data (NARR from the US National Oceanic and Atmospheric Administration – NOAA) and the ERA-Interim Reanalysis 6-hr temperature data (European Centre for Medium-Range Weather Forecasts – ECMWF) available for the specific grid points [4.875°, -75.375°] and [4.75°, -75.375°] of the northern Andes. NARR and ERA-Interim data both comprised the

historical period spanning from January 1979 to the present. We processed ECHAM4.5 mean monthly near-surface and free air temperatures (Roeckner et al. 1996) for the same set of grid points representing the axis of the Andes cordillera and for the period spanning from January 1950 to December 2016. We selected the ECHAM4.5 General Circulation Model (GCM) because it shows, in most of the tropical belt 15°S-12°N, the highest correlation coefficients between observed near-surface temperatures anomalies and the corresponding simulation outputs for the historical period 1950-2000.

3.5 Ground-truth air temperature data

We analyzed ground-truth near-surface air temperature daily data of the set of meteorological stations located in the surroundings of the El Ruiz-Tolima volcanic massif. In total, ten quality-controlled weather stations located within the [04°25'-05°15'N and 75°00'-76°00'W] spatial domain were selected. These weather stations are operated by the Colombian meteorological service (the Instituto de Hidrología, Meteorología y Estudios Ambientales – IDEAM) and the Colombian Coffee Research Center (the Centro de Investigaciones del Café – CENICAFÉ), and their instrumental periods range from 21 years (the shortest historical period) to 58 years (the longest dataset). We also processed the hourly records gathered at a set of temperature and humidity data loggers that we installed in late 2008 (Ruiz et al. 2011; Ruiz-Carrascal 2016) along an elevational gradient that follows the main stream of the Claro basin. In total, twelve digital sensors (out of twenty-three U23-001 HOBO® data loggers) were selected for this analysis. Even though hourly near-surface ambient temperatures comprise historical periods as long as thirteen years (from mid-December 2008 to the present), the common, homogenous, and continuous instrumental period spans from December 2013 to the present.

4   Methods

Fig. 2-A and Fig. 2-B show the simplified East-West atmospheric circulation patterns in the equatorial troposphere along a representative latitude (5°N). A schematic diagram of the method implemented here to reconstruct past fluctuations of

the FLH in the two sites of interest is shown in Fig. 2-C. Upward and downward shifts of the FLH are controlled by changes in the intercept and slope parameters of the straight line that represents the altitudinal behavior of the free air temperature in the troposphere. Hence, four aspects are needed in our analysis: changes in SSTs, changes in mean sea level, and normal distribution of air-sea temperature difference in areas where deep convection occurs, which together are behind changes in the intercept, as well as changes in the Environmental Lapse Rates (ELRs), which represent the fluctuations of the slope parameter. Note that the spatio-temporal dynamics of both the Indo-Pacific and Atlantic oceans need to be considered, because these two ocean basins play a key role in the regional atmospheric circulation dynamics (particularly in Walker circulation dynamics) during the different ENSO phases.

For the purpose of our research, we began our analysis with detailed remote sensing and field-based moraine mapping. To estimate fluctuations in near-surface air temperature at sea level over the past 30 kyr, we processed paleo-reconstructed SSTs and relative sea levels in the Indo-Pacific and Atlantic oceans, as well as present-day SSTs in key areas of their equatorial portions. We also analyzed reanalysis and GCM data to quantify present-day ELRs in the areas of interest and merged them with the main modes of variability of sea surface temperatures anomalies to infer past potential conditions. In summary, the following six main steps were followed: (1) remote sensing and field-based geomorphological mapping; (2) processing of paleo data; (3) analysis of historical SST data; (4) processing of reanalysis and GCM data; (5) inference of past ELRs; and (6) final integration of our findings. A brief description of these methodological steps is presented below. Additional
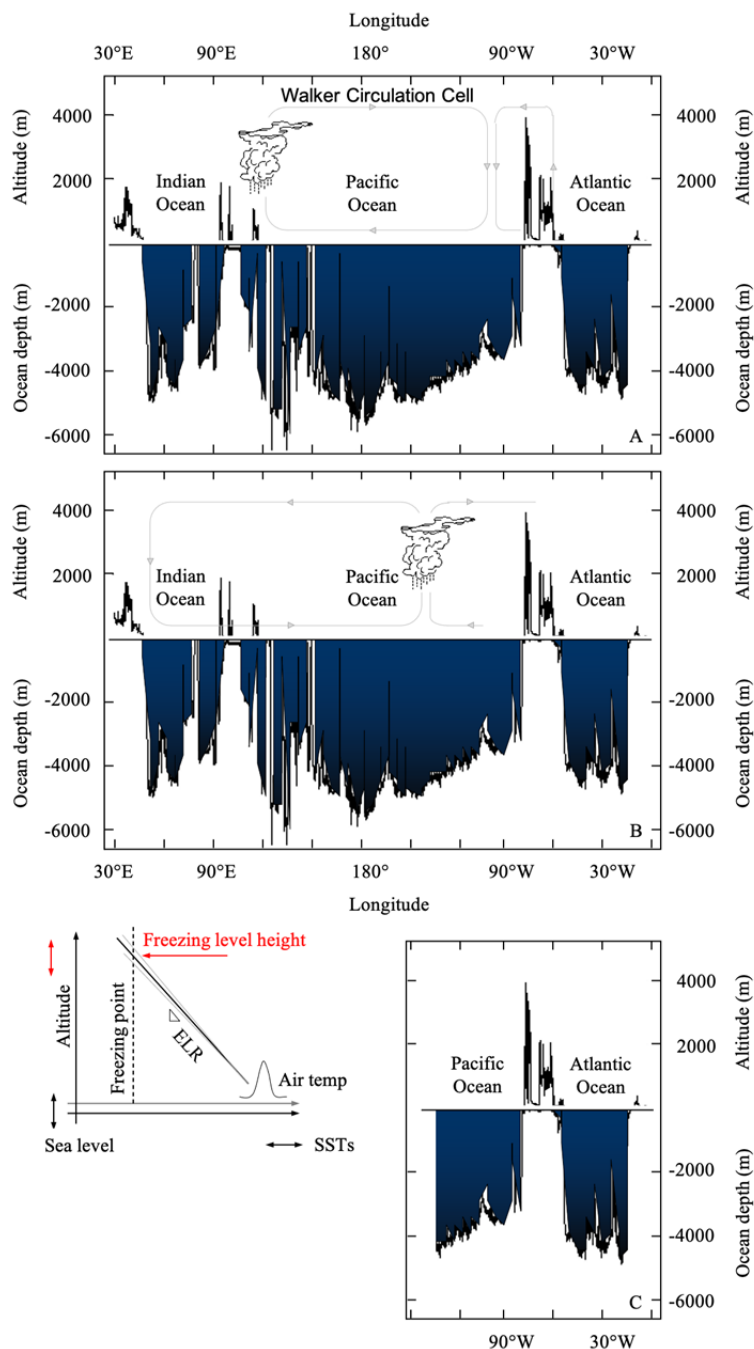

Fig. 2 Topographic profile along a 5°N zonal transect extending from 30°E to the Greenwich Meridian. (A) December-January-February (DJF) East-West circulation in the equatorial troposphere during normal conditions. (B) DJF East-West circulation during El Niño-like conditions. The black solid line depicts the ground surface (above the mean sea level) and the ocean bottom (below the mean sea level) along the 5°N transect. The gray solid lines and the blue shaded areas represent the circulation cells and the oceans, respectively. (C) Schematic diagram of the method implemented and data required (left sketch) to assess long-term fluctuations in the freezing level height. Inferred altitudes of the 0°C isotherm are projected on the upper ranges of the Andes Cordillera – see sketch to the right.

information and details can be found in the Online Resource.

4.1 Remote sensing and field-based geomorphological mapping

~0.3-m Bing satellite images were processed to identify moraine units, glacier lakes, cushion bogs, and cirques. Landforms in Los Nevados also included lava flow scarps. Surface geomorphic maps were produced during the photointerpretation process. Field trips to the main study site were conducted to validate our findings and complete the mapping. The resulting ground-truthed geomorphological map was then compared with previously published reconstructions of glacier advances.

4.2 Processing of paleo data

Paleo-reconstructed SSTs and relative sea levels of the eastern tropical Pacific were integrated into single time series plots spanning 30 kyr. The phases of glacier expansion reported in the literature (Thouret et al. 1996), during which mountain glaciers in the Ruiz-Tolima volcanic massif likely reached the maximum extent of their ice margins, were highlighted in time series plots. Present-day SSTs suggested by the paleo-reconstructions were compared with the annual cycles of SSTs observed in the Niño 1+2 and Niño 3.4 regions of the eastern and central tropical Pacific.

4.3 Analysis of historical SST data

Kaplan's SSTa gridded datasets were decomposed into combinations of orthogonal spatial patterns with corresponding principal components (PCs) by implementing the Singular Value Decomposition/Empirical Orthogonal Function-EOF analysis (Lorenz 1956). Only the first leading modes of spatio-temporal variability (EOF modes) and PCs were used herein because: (a) they explain most of the spatio-temporal variability of SSTa fields; and (b) previous studies (e.g., Mölg et al. 2017) have pointed to strong linkages between the intensity of El Niño Southern Oscillation and surface mass balance changes in the Santa Isabel nevado. NOAA NCDC ERSST version2 SST data were used to analyze the spatial distribution of grid points (and the corresponding yearly climatology) that have SSTs above the minimum temperature necessary to initiate deep convection (300 K; Ramanathan and Collins 1991).

4.4 Processing of reanalysis and GCM data

3-hr NARR and 6-hr ERA-Interim free air temperatures were processed to assess the vertical profiles of ambient temperatures at a monthly timescale. Linear regressions were adjusted, and the resulting slope parameters (mean monthly environmental lapse rates, ELRs) were compared with ground-truth data, which were obtained through the analysis of daily near-surface mean air temperatures. Wavelet analysis was implemented to assess the main dominant signals in ERA-Interim standardized time series of ELRs. Simple correlation analyses between ERA-Interim ELRs and Kaplan's SSTa for a 0-month time lag were conducted to highlight areas within the Indo-Pacific and tropical Atlantic Ocean basins with correlation coefficients (R-values) higher than a +0.5 threshold. Near-surface air temperatures suggested by Reanalysis-2 data were combined with LEVITUS94 monthly SSTs to assess the normal seasonal distribution of air-sea temperature differences in the tropical Pacific and tropical Atlantic oceans. Scatter plots of 0-, 1-, 2-, and 3-month lagged ERA-Interim ELRs versus Indo-Pacific and tropical Atlantic *eigenvalues* were plotted, and linear trends with corresponding ±1.0 standard deviation were adjusted. Scatter diagrams were compared with the frequency histogram of ERA-Interim ELRs for the full historical period 1979-2017. Correlation coefficients and slope parameters between ERA-Interim ELRs and Indo-Pacific and tropical Atlantic *eigenvalues* were then plotted on radar charts.

ECHAM4.5 and Reanalysis-2 gridpoints along the axis of the Andes Cordillera were obtained by masking the NOAA NGDC GLOBE gridded 1-km global DEM with their grids. EOF analysis was implemented to assess the main modes of spatio-temporal variability of ECHAM4.5 and Reanalysis-2 near-surface and free air temperature gridded datasets. Only the first EOF modes and PCs were considered.

4.5 Inference of past ELRs

Potential values and ranges of past ELRs in the main study site were inferred using two complementary approaches: (i) restricting the ELR interval to values consistent with present-day moist

adiabatic lapse rates observed in the upper ranges of each mountain range; and (ii) assuming ELR values based on present-day relationships observed in the scatter diagrams of ERA-Interim ELRs vs. equatorial Pacific and tropical Atlantic *eigenvalues*.

4.6 Final integration of our findings and reconstruction of the FLH

Paleo-reconstructed SSTs, relative sea levels, air-sea temperature differences, and inferred ELRs were used to reconstruct the FLH. Inferred fluctuations of the FHL were plotted on 30-m digital elevation models of the Ruiz-Tolima volcanic massif and the Sierra Nevada del Cocuy and compared with on-the-ground corrected geomorphological maps.

5 Results

5.1 Time-series reconstruction

Fig. 3 shows our inferred altitudes of the FLH for the main study site. The phases of glacier expansion suggested by Thouret et al. (1996) for the Ruiz-Tolima volcanic massif are highlighted with vertical dashed lines. These phases include: (A) Early Murillo, 28-21 kyr, early to middle full glacial interval, the most voluminous glacial deposits. Note that in the article by Palacios et al. (2020), the authors refer to the global Last Glacial Maximum – gLGM as the time period spanning from 26.5 to 19 kyr (Clark et al. 2009). They also call the Last Glacial Termination the time period between the gLGM and the beginning of the current interglacial period, the Holocene. (B) Late Murillo, 21-14 kyr, commonly assumed as the LGM limit; interestingly, mountain glaciers in the equatorial Andes 'had already retreated dramatically during late-full glacial' (Thouret et al. 1996). (C) Early Otún, 13-12.4 kyr, potentially related to the Antarctic Cold Reversal (14.6 to 12.9 kyr), termed the Bølling-Allerød interstadial in the northern hemisphere. Note that the Lateglacial, ~16.7 and 11.5 kyr, defined in the article by Rodbell et al. (2009), comprises a part of the Late Murillo and the full extent of the Early Otún. (D) Late Otún, 11-10 kyr, correlated with the Younger Dryas Stadial on the Northern North Atlantic region; 12.85-11.65 kyr. (E) Early Santa Isabel, 8.6-7.4 kyr, related to the 8.2 kyr event. (F) Late Santa Isabel, 7.4-6.2 kyr, embedded in the Holocene Thermal
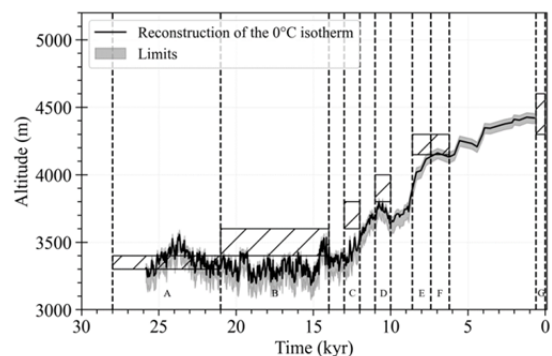

Fig. 3 Inferred altitudes of the freezing level height in the headwaters of the Claro river basin, on the northwestern flank of the Ruiz-Tolima volcanic massif in the Colombian Central cordillera. The solid line depicts the inferred mean value. The gray shading represents the upper and lower limits. The striped boxes depict the ranges of heights suggested by Thouret et al. (1996) for past glacier-front advances – see main text.

Maximum – HTM (10-5 kyr). And, (G) Early Neoglacial, 0.6 kyr to present-day, comprising the Little Ice Age – LIA (1450–1850 C.E.). Older cold stades not shown here include: >48 kyr (Early Rio Recio stade) and 48-33 kyr (Late Rio Recio stade).

In our study, the maximum extents of ice margins on the west flank of the Ruiz-Tolima volcanic massif seem to be better represented with a single, merged time series of reconstructed eastern tropical Pacific SSTs. The individual Bova et al. (2015) paleo-reconstruction provides a good approximation for the formation of glacier tongues over the period spanning from the Early Murillo stade to the Late Otún stade. The past ice margins of the Early Santa Isabel and the Late Santa Isabel could be better inferred with the individual Kienast et al. (2006) paleo-reconstruction, whereas Early Neoglacial advances could be well represented with the individual Dyez et al. (2016) paleo-reconstruction. As an example of individual inferences, the Bova et al. (2015) paleo-reconstruction of eastern tropical Pacific SSTs allows inferring a likely altitude of the FLH in the range from 3,280 to 3,480 m (i.e., a mean of 3,380 m) during the Late Murillo stade, consistent with field observations and previous publications. These FLHs are 440 to 520 m and 280 to 400 m lower than the FLHs that could be inferred with Dyez et al. (2016) and Kienast et al. (2006) paleo-reconstructions, respectively, which suggest FLHs falling in the ranges from 3,800 to 3,920 m, and from 3,560 to 3,880 m. Conversely, the individual Bova et al. (2015) paleo-reconstruction

suggests a present-day FLHs located at a very low altitude of about 3,960 m, differing in about 320 to 440 m from the Dyez et al. (2016) and Kienast et al. (2006) paleo-reconstructions, which suggest snowlines at around 4,280 and 4,400 m, respectively.

Table 1 shows a comparison between the FLHs inferred in this study for the headwaters of the Claro river basin and the main glacier-front advances suggested by Thouret et al. (1996). Our estimates indicate that the overall lowest average FLH reached an altitude of 3,280 m with a lower limit of 3,150 m during the Early Murillo cold stade, when most voluminous glacial deposits were accumulated in the Ruiz-Tolima volcanic massif. Such an altitude is consistent with previously-reported lowest glacier-front advances (3,250 m). During the most recent cold stade, i.e., the Early Neoglacial, the FLH likely reached an altitude of 4,400 m with a lower limit of 4,380 m. Such an altitude is 150 m below the lowest altitude of 4,550 m of the ice-cap margins previously suggested for the Little Ice Age, 1450-1850 C.E. Table 2 shows similar comparisons for the comparative site, the Lagunillas river in the Sierra Nevada del Cocuy. In general, our inferences of the average lowest altitude of the FLH are consistently above the main glacier-front advances suggested by van der Hammen et al. (1980/1981). The altitudinal difference reaches 550 to 650 m during the Early Lagunillas cold stade, 21 to 14 kyr, and 500 to 550 m during the Late Lagunillas, 13 to 12.4 kyr. In the recent cold stades, i.e., Bocatoma (11 to 10 kyr) and Corralitos (1500 to 1850 C.E.), the altitudinal difference is about 600 to 400 m and 150 to 350 m, respectively.

5.2 Remote sensing and field-based geomorphological mapping

A vast array of geomorphological features was found in the headwaters of the Claro river basin. Landforms include multiple water body types (glacier lakes, small lagoons, cushion and peat bogs), lava flow scarps, cirques, lahar deposits, and moraine units (Fig. 4). Water bodies in the area are restricted to altitudes above 4,050 m and have surface areas that vary throughout the year but never exceed 0.4 km². Remnants of past glacial lakes and present-day

Table 1 Comparison between the average freezing level heights inferred in this study for the headwaters of the Claro river and the corresponding main glacier-front advances suggested by Thouret et al. (1996). The key six periods discussed by Jomelli et al. (2014) and Palacios et al. (2020) are included at the bottom of the table for reference.

Cold stade	Average altitudinal range (m)	
	FLH inferred in this study	Glacier-front advances suggested by Thouret et al. (1996)
(A) Early Murillo, 28 to 21 kyr$	3,280 to 3,560 (High uncertainty)	3,250 to 3,700
(B) Late Murillo, 21 to 14 kyr%	3,240 to 3,560 (High uncertainty)	3,500 to 3,800
(C) Early Otún, 13 to 12.4 kyr	3,360 to 3,560	3,500 to 3,700
(D) Late Otún, 11 to 10 kyr&	3,680 to 3,800	3,900 to 4,400
(E) Early Santa Isabel, 8.6 to 7.4 kyr	3,800 to 4,160	--
(F) Late Santa Isabel, 7.4 to 6.2 kyr	4,160 to 4,180	4,400 to 4,550
(G) Early Neoglacial, 0.6 kyr to present-day	Lowest altitude 4,400	Lowest altitude 4,550

Notes: $ Pre-ACR (>14 kyr) (Jomelli et al. 2014); gLGM (26.5-19 kyr) (Palacios et al. 2020)

% ACR (14.6-12.9 kyr) and YD (12.8-11.5 kyr) (Jomelli et al. 2014); HS-1 (17.5 to 14.6 kyr), ACR (14.6-12.9 kyr), and YD (12.9-11.7 kyr) (Palacios et al. 2020)

& Early Holocene (11.7 to 7 kyr) (Palacios et al. 2020)

Table 2 Comparison between the average freezing level heights inferred in this study for the headwaters of the Lagunillas river and the corresponding main glacier-front advances suggested by van der Hammen et al. (1980/1981).

Cold stade	Corresponding cold stade in the Ruiz-Tolima volcanic massif	Average altitudinal range (m)	
		FLH inferred in this study	Glacier-front advances suggested by van der Hammen et al. (1980/1981)
(I) Cóncavo, 27 to 25 kyr	First half of (A) Early Murillo	Not defined	3,000 to 3,400
(II) Early Lagunillas, 21 to 14 kyr	(B) Late Murillo	3,850 to 4,050	3,300 to 3,400
(III) Late Lagunillas, 13 to 12.4 kyr	(C) Early Otún	3,800 to 3,950	3,300 to 3,400
(IV) Bocatoma, 11 to 10 kyr	(D) Late Otún	4,500 to 4,600	3,900 to 4,200
(V) Corralitos, 1500 to 1850 C.E.	(G) Early Neoglacial	ca. 4,650	4,300 to 4,500

cushion bogs are confined by many moraine deposits which serve as their natural dams. Even though documenting geological processes associated with recent volcanic activity of the El Ruiz, Santa Isabel and El Cisne (already disappeared) nevados was beyond the scope of this study, we found necessary to map lava flows and scarps because many of these forms can be mistakenly interpreted as moraines in satellite images (Fig. 5-A). Lava flows and escarpments create a noticeable genetic-depositional control where cirques, moraines, lakes, and other elements typical of glacial activity form. The high slopes of lava flows restrict ice deposits, and thus potential accumulation zones were found only in the ground right below lava scarps.

Around ten cirques were identified in the headwaters, restricted to the altitudinal range [4,000-4,600 m]. They are located right above genetically-related moraines. Their concave shapes reach diameters ranging from 500 to 800 m in length. Although cirques are formed under mainly topographic controls, some of these landforms are

Fig. 4 Images of some geomorphological landforms in the headwaters of the Claro river. A-Tephra deposits over an unconsolidated glacial debris. B-Tephra deposits over a moraine outcrop. C-Moraine deposit confining a cushion bog. D-Well-preserved, vegetation-free, frontal moraine with no soil and ash deposits on top. E-Lava flow scarp and a cirque typical morphology.

genetically favored by lava flow scarps. Three lahar deposits were also identified, all of them in the altitudinal range [4,300-4,600 m]. They are restricted to the northwestern flank of the Santa Isabel Nevado (the slope that separates it from the El Ruiz Nevado, located to the north). These deposits are elongated bodies whose orientation is aligned with the axis of the basin and are not controlled by the orientation of the two nearby peaks. Lateral moraines were deposited on top of these lahar deposits, which implies that (in a relative chronology of events) there were moments of glacial cooling that allowed the advance of glacier fronts over older lahar deposits. Lastly, frontal moraines were found to be restricted to altitudes above 3,900 m (for reference, the present-day ice margin is located at an altitude of 4,750 m). Lateral moraines are more abundant than frontal moraines, and are observed along the glacial valley outlets in the altitudinal range [3,300 to 4,600 m]. Systems or swarms of small moraines occur mainly above 4,100 m, while below this altitude moraines are more isolated and with a lower density of occurrence. There are a few occurrences of complete moraine systems in which it was possible to identify the terminal, frontal, and lateral moraine of the same event: only five systems allowed the reconstruction of a glacial paleo-tongue. In the comparative site in the Sierra Nevada, landforms of our interest include moraine units and cirques (Fig. 5-B).

Fig. 6-A depicts the inferred spatial distribution of the reconstructed altitude of the 0°C isotherm in the main study site alongside the set of moraines and lahars that were identified in our interpretation process. For the sake of comparison, the main phases of glacier expansion suggested by Thouret et al. (1996) are shown in Fig. 6-B. Comparative maps for individual cold stades (specifically, Early Murillo, Late Murillo, Late Otún, and Late Santa Isabel) are presented in the Online Resource. In general, the potential extent of ice-caps suggested here exceeds in area the corresponding glacier front advances proposed by Thouret et al. (1996). The greatest differences are observed in the cold stades Late Murillo and Late Santa Isabel. Our inference of the FLH for the Late Murillo cold stade (3,240 to 3,560 m) is 260 to 240 m lower than the [3,500-3,800 m] altitudinal range previously suggested. Our estimate of the average FLH during the Late Santa Isabel cold stade, 7.4 to 6.2 kyr, when a vast number of moraine units in the main study site were deposited, reach
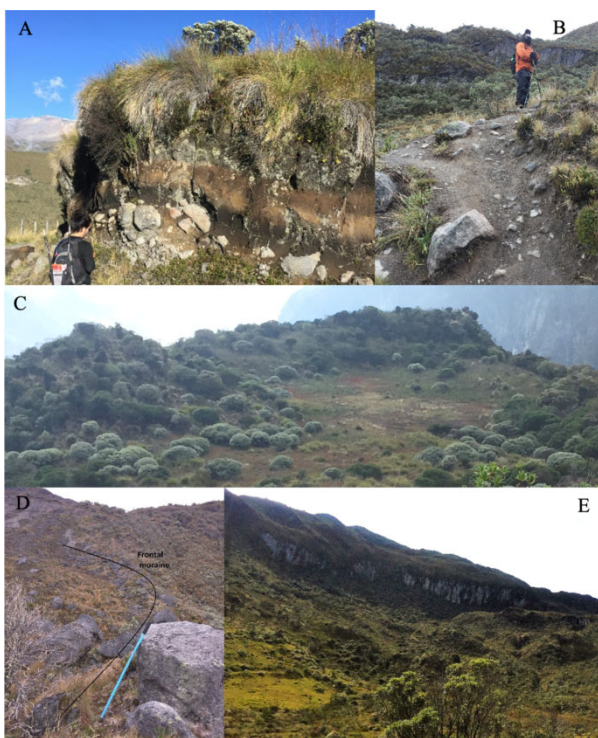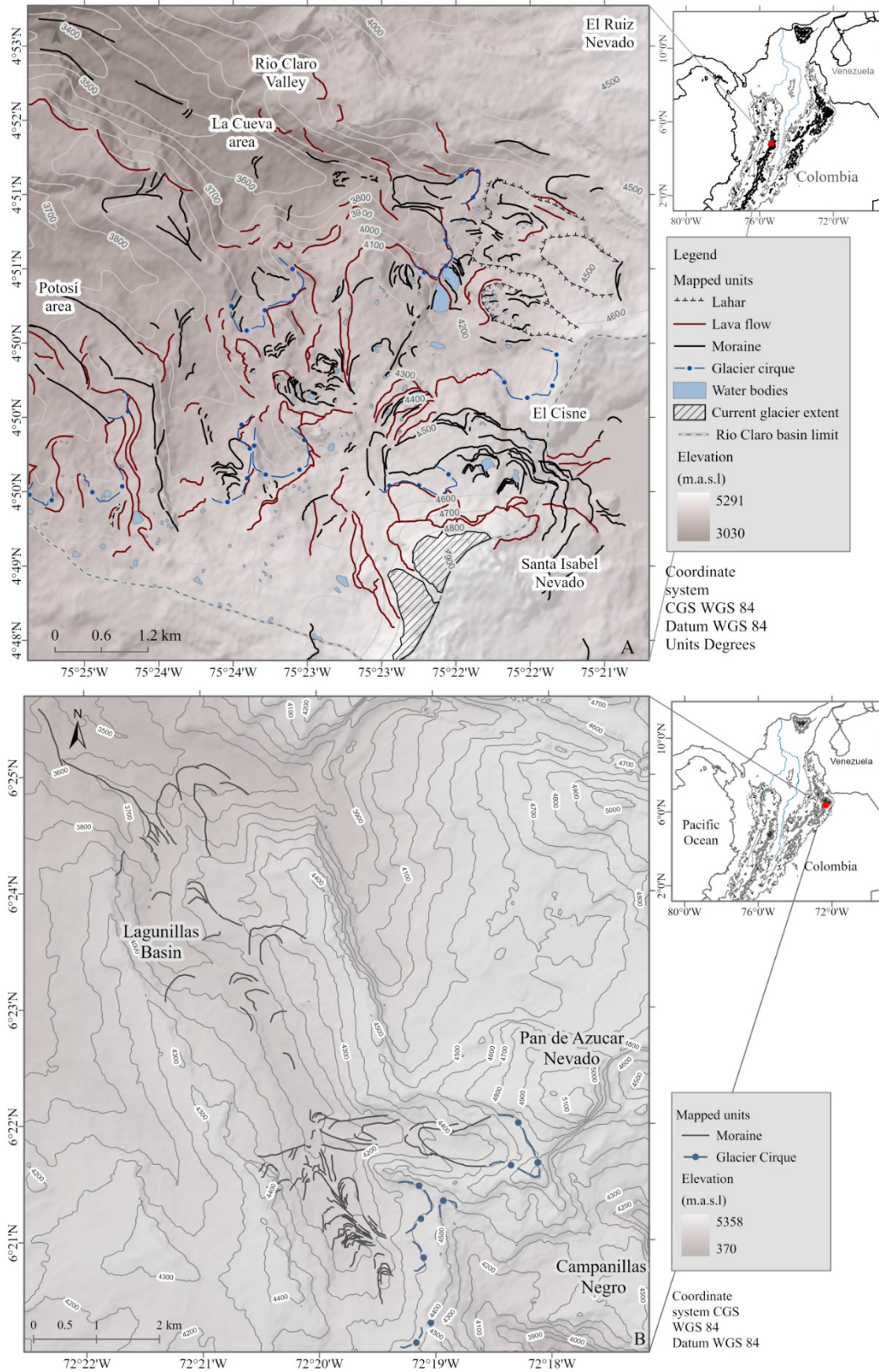
Fig. 5 Maps of geomorphological landforms. (A) Headwaters of the Claro river. (B) Headwaters of the Lagunillas river (in this case, only moraine units and cirques are plotted).
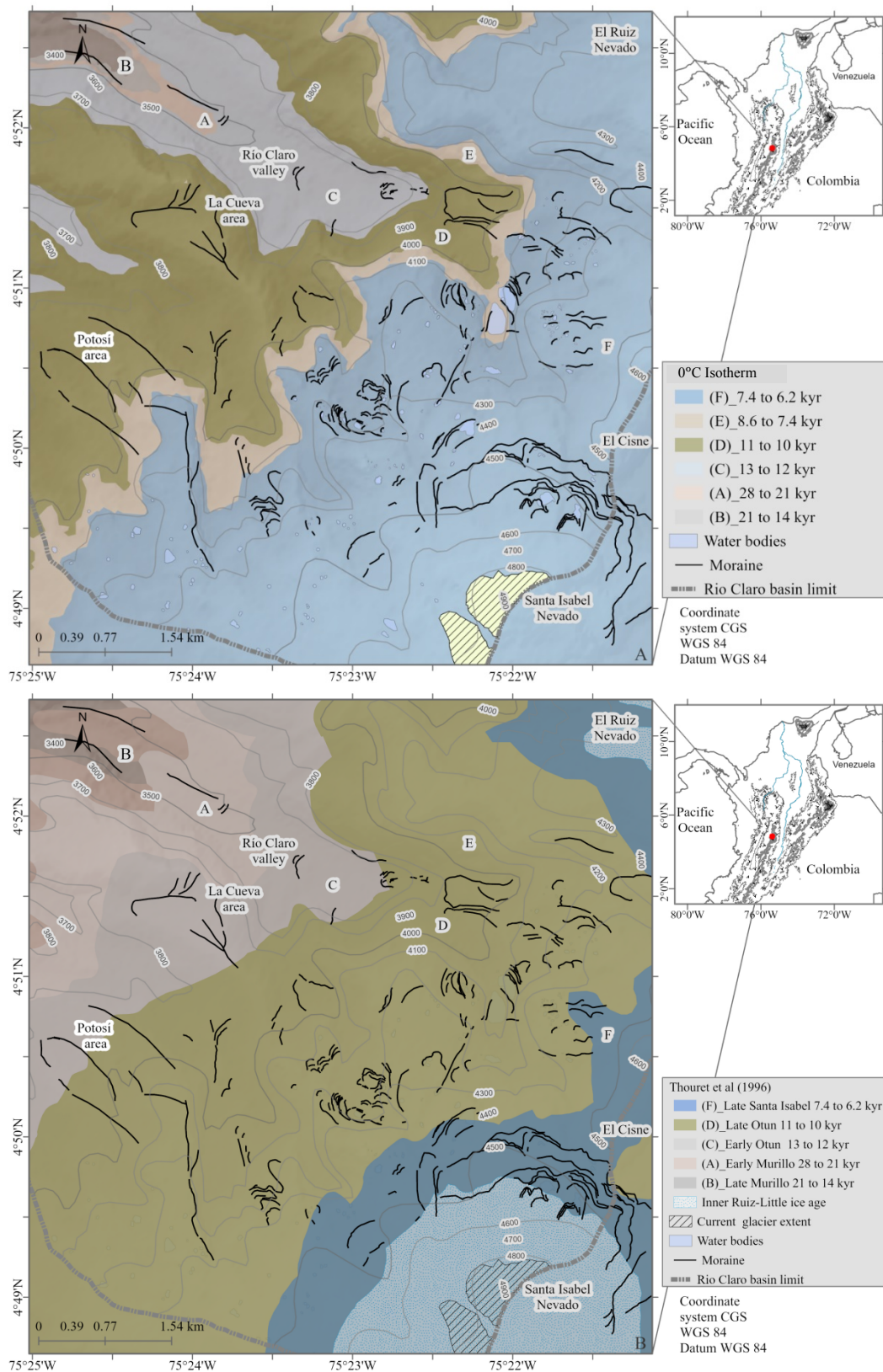
Fig. 6 Likely average lowering of the FLH in the Claro river high-mountain basin (A) compared with glacier-front advances suggested by Thouret et al. (1996) (B). Only glacial landforms are displayed here. Contours lines are displayed to facilitate the reading of the altitude of terminus moraines. Uppercase letters A to F depict the phases of glacier expansion suggested by Thouret et al. (1996) for the Ruiz-Tolima volcanic massif.

altitudes in the range from 4,160 to 4,180 m with a lower limit of 4,120 m. Such altitudes are 240 m below the lowest altitude reached by glacier-fronts suggested by Thouret et al. (1996). There is also a significant difference in the set of contours inferred with our approach: as expected, the FLHs match the topography of the headwaters of the basin under study, compared to the glacier front advances suggested by previous studies which descend along valley outlets.
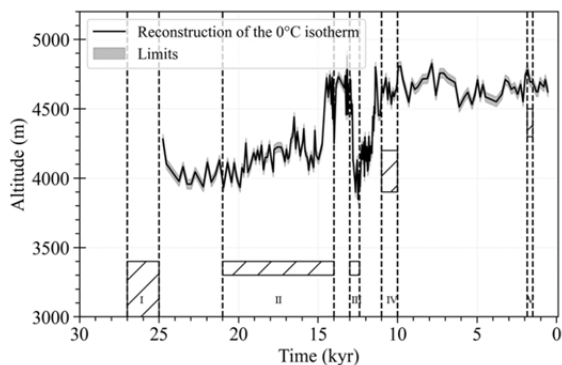

Fig. 7 Likely average lowering of the FLH in the southwestern flank of the Sierra Nevada del Cocuy. The solid line depicts the inferred mean value. The gray shading represents the upper and lower limits. Phases of glacier expansion in the Sierra Nevada (van der Hammen et al. 1980/1981) are highlighted with vertical dashed lines: (I) Cóncavo, 27 to 25 kyr; (II) Early Lagunillas, 21 to 14 kyr; (III) Late Lagunillas, 13 to 12.4 kyr; (IV) Bocatoma, 11 to 10 kyr; and (V) Corralitos, 1500 to 1850 C.E. The striped boxes depict the ranges of heights suggested by van der Hammen et al. (1980/1981) for past glacier-front advances.

Fig. 7 shows our inference of the past 0°C isotherms in the headwaters of the Lagunillas river basin. The interpreted (via remote sensing) cirques and moraine units for this comparative site are shown on the local map (Fig. 8). Since the average lowest altitude of the FLH proposed here is consistently above the main glacier-front advances suggested by van der Hammen et al. (1980/1981), our resulting potential areal extent of ice-caps is significantly smaller than their inferences. Significant differences between the Early Santa Isabel, the Late Santa Isabel, and the Early Neoglacial cold stages obtained for the El Ruiz-Tolima volcanic massif are not observed in the Sierra Nevada del Cocuy. The FLH inferred here for the Early Neoglacial (up to 4,650 m) is significantly higher than the outermost bordering moraine (ca. 4,450 m), located in the upper part of the Bocatoma Valley, of the Corralitos cold stade of

Sierra Nevada (V; 1500 to 1850 C.E.). The FLH inferred for the Late Otún in the El Ruiz-Tolima volcanic massif, which corresponds to the Bocatoma cold stade in the Sierra Nevada (IV), could have reached an altitude of about 4,500 m. Such an altitude is 500 m higher than the altitude of the Bocatoma moraine (ca. 3,950 m), which is located right at the junction of the Bocatoma and Lagunillas valleys (van der Hammen et al. 1980/1981), and that was suggested to be ca. 11,000 to 10,000 years old. Lastly, the FLH proposed herein for the Early Otún in the El Ruiz-Tolima volcanic massif, which corresponds to the Late Lagunillas cold stade in the Sierra Nevada (III), could have reached an altitude of 3,800 m. This altitude is in the close surroundings of the location of the Upper Lagunillas moraine (ca. 3,900 m), which was suggested to have lasted from ca.13 to 12.4 kyr.

6 Discussion

The main study site, the Claro river high-altitude basin on the El Ruiz-Tolima volcanic massif in the Colombian Central cordillera, has been subject to multiple geological processes, such as the deposition of volcanic ashes and pyroclastic debris, lahar flows and erosion, which have contributed to the masking of unconsolidated glacial debris, the burying of moraine systems and the loss of medial and terminus moraines. Therefore, it was difficult to recognize and delineate paleo-ELAs in the set of moraine units we identified during our photointerpretation and geomorphological field mapping. In order to infer potential glacial advances during past cold stages, our handy alternative was to calculate the different paleo-altitudes of the 0°C isotherm. We replicated the methodology in a comparative site, the Lagunillas river basin, which is located on the southwestern flank of the Sierra Nevada del Cocuy, in the Eastern cordillera. Fluctuations of the paleo-altitudes of the Freezing Level Height were plotted on high-resolution digital elevation models of each site, and the corresponding cartographic maps were validated with previously-published geomorphological maps. The combined maps of glacial landforms and 0°C isotherms are providing us with a well-founded reconstruction of potential Late Pleistocene to Holocene glacial advances in the headwaters of the Claro river. Our inferences match some of the critical features of the six key periods widely explored in the

scientific literature (Palacios et al. 2020):

(1) The global Last Glacial Maximum – gLGM, 26.5-19 kyr (Clark et al., 2009), when temperatures were 6 to 8°C colder than present-day conditions. For the site in the Central Cordillera, our inferred FLHs reach a likely altitude that is 1,820 to 1,540 m below the modern, estimated FLH. These altitudinal differences are consistent with, but exceed the average difference of paleo-ELAs (~1,300 m lower) suggested for the Eastern Cordillera with respect to modern ELAs (Palacio et al. 2020). Our inferred FLHs also exceed the predicted 1,350 m ELA decrease for a uniform drop of temperature of -6°C (Sagredo et al. 2014). The 520 to 240 m difference between the inferred FLH and the suggested paleo-boundary between the zones of net accumulation and net ablation is reasonable given the overall characteristics of the glacial valley outlets in the Claro river headwaters. For the comparative site in the Eastern cordillera, we do not have estimates.

(2) The Heinrich Stadial 1 – HS-1, also called the 'Oldest Dryas' in Scandinavia, which extended from the Heinrich 1 "event," 17.5 kyr, to the beginning of the Bølling-Allerød Interstadial, 14.6 kyr. During this period, the northern Andes experienced cold temperatures (but higher than during the LGM) and great variability of the ELA. Our inferences for the main study site point to a rapid descend of the FLH from 16 to 15 kyr, followed by a faster uplift from 15 to 14 kyr. The lowest altitude likely reached by the 0°C isotherm was 1,980 to 1,860 m below the modern, estimated FLH. Such rapid cooling may have brought the conditions for glaciers thickening and advances in the area, which was suggested to take place around ~18-15 kyr according to [10]Be ages (Palacios et al. 2020). Note that our inferences point to a FLH that was 160 to 320 m lower during the HS-1 than during the gLGM but for a short period of time. Only the study by Thouret et al. (1996) provides us with a comparative age through their assessment of a peat overlying a moraine complex (precise altitude unknown) which yielded a minimum age of 16-15 kyr. For the study site in the Sierra Nevada, our inferences indicate a potential altitude of the FLH of ~4,000 m, almost 1,000 m above the moraine complex in the Sabana de Bogotá (precise altitude unknown) that was dated to between 18 and 14.5 kyr.

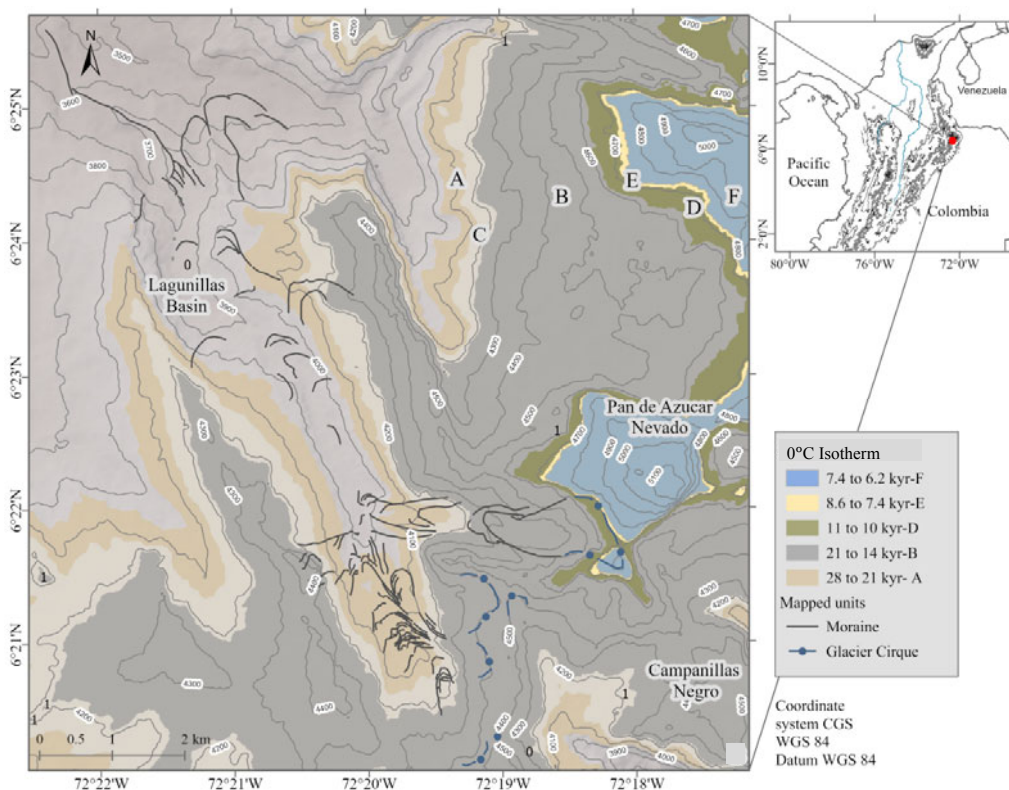*(3) The Bølling-Allerød Interstadial – B-A, 14.6-*

Fig. 8 Map of FLHs in the headwaters of the Lagunillas river. Phases of glacier expansion suggested by Thouret et al. (1996) for the Ruiz-Tolima volcanic massif (upper case letters A to F) are shown here as a reference and for the sake of comparison.

12.9 kyr, a warm period, mostly in the northern hemisphere, during which a northward migration of the Intertropical Convergence Zone (ITCZ) likely took place. Our inferences of past changes in the FLH in the main study site indicate a stable period starting at ~14 kyr and extending until ~13 kyr, followed by faster warming that ended ~11 kyr. For the study site in the Sierra Nevada, our estimates suggest that the stable period abruptly came to an end ~13 kyr and was subsequently followed by fast cooling that extended for almost 500 yr; i.e., it ended ~12.5 kyr.

(4) *The Antarctic Cold Reversal – ACR, 14.6-12.9 kyr, a mostly southern hemisphere climatic signal. Many glaciers in the tropical Andes advanced during this period, owing to a clear cooling signal in high altitude Andean regions (temperature in the region reached values 2.9±0.8°C lower than today).* Our inferences for the main study site in the Central Cordillera do not point to a FLH lowering that may have driven readvances of glacier tongues during the ACR. Recent literature (Rodbell et al. 2009) suggests that the Late Otún moraines (11-10 kyr; Thouret et al. 1996) in the Central Cordillera are older than ~14,5 kyr. Three samples in this unit yielded minimum limiting ages ranging from 14.440 to 14.480 (+0.170) kyr (+1s), and one sample yielded a maximum limiting age for Late Otún moraines of 15.360-16.690 kyr. Our estimates for the comparative site in the Sierra Nevada indicate, on the contrary, that the fast cooling mentioned above could have caused significant advances between 13 and 12.4 kyr. This statement agrees with previous research efforts that point to several advances or stillstands during the ACR. Specifically, Jomelli et al. (2014) argue that the Ritacuba Negro glacier in the Sierra Nevada reached the maximum glacial extent of the late glacial during the ACR, forming moraines at altitudes ca. 3,975 m around 13.9±0.3 [10]Be kyr ago. This advance is linked to a paleo-ELA decrease of about 500 m. In summary, our estimates suggest that only the comparative site in the Sierra Nevada was sensitive to the ACR southern hemisphere signal.

(5) *The Younger Dryas – YD, 12.9-11.7 kyr, a cold interval (2.2 to 3.8°C colder than today), characterized by a southward migration of the ITCZ and (overall) small advances of glaciers in northern South America.* In general, the scientific literature now argues that glaciers in the northern Andes reached a larger extent during the ACR (discussed above) than during the YD (Jomelli et al. 2014).

Nevertheless, some evidence suggests that a stronger YD connection, particularly in latitudes from 0 to 9°N, may exist (Rodbell et al. 2009). Our inferences for the main study site only point to a cooling event during the period 11-10 kyr, well after the end of the YD cold interval. For the comparative site in the Sierra Nevada, our estimates suggest a rapid lowering of the FLH between 11.4 and 11 kyr, again after the end of the YD. This cooling could be supported by previously-published glacier advances in the Sierra Nevada del Cocuy and on the Sabana de Bogotá (Palacios et al. 2020), which are related to events that likely took place at the very end of the YD, 11.8±0.2 kyr (Jomelli et al. 2014), and contradicts the rapid warming suggested by Kaufman et al. (2020) for 12 to 10 kyr. In summary, none of our study sites show lowering of the FLH during the YD. The downward shifts in the FLH in our main and comparative study sites took place about 0.7 to 0.3 kyr after the end of the YD, respectively, and the shifts were of about 240 m and 360 m, respectively. The latter lowering in the Sierra Nevada represents ca. 39% of the total 920-m downward shift during the ACR.

(6) *The Holocene, c. 11.7 kyr to present.* Our inferences for the main site point to overall rapid warming with two reversal periods: from 7 to 6.2 kyr and from 5.5 to 4.5 kyr. None of the cooling periods have been reported previously. Furthermore, the first period overlaps the warmest millennium of the Holocene (centered on 6.5 kyr) that has recently been suggested (Kaufman et al. 2020) through the assessment of the 0-30°N reconstructed time series of mean surface temperatures of the past 12,000 years. For the site in the Sierra Nevada, our estimates point to multiple periods of rapid cooling, which took place along a long-term stable condition over the entire Holocene. The most prominent periods include 10-9 kyr, 7.5-6 kyr, 4-2.5 kyr, and 2-1.0 kyr. None of them, except the last one, have been discussed before (Neoglacial advances in the interval 2.5-1.0 kyr in Rodbell et al. 2009). Even though ~450 yr Little Ice Age moraines have been observed in all glacierized mountain ranges in the northern Andes (Rodbell et al. 2009), our assessment is limited by the temporal resolution of our analyses, and thus recent cooling periods are not captured.

The likely altitudes of the FLH proposed here for the headwaters of the Claro river basin also follow the general tendency of the time series of temperature difference (from the present) from the Vostok ice core

and the ^{18}O/^{16}O isotopic ratio from the Greenland Ice-core Project – GRIP, as shown in the Online Resource. The fluctuations of these time series correspond to the well-known periods (e.g., gLGM, HS-1, ACR, YD, etc.) mentioned above. In terms of variability, and due to the higher fluctuations of the GRIP data, the likely altitudes of the FLH tend to march with the ups and downs of the ^{18}O/^{16}O isotopic ratio series, particularly during the Early Murillo cold stade. There are important differences from the Late Murillo cold stade to the present, except for the rapid warming in the last millennium of this stade and the climatic reversal during the Early Otún.

By comparing our velocity inferences with the only available glacial records for the Ruiz-Tolima volcanic complex and the Sierra Nevada del Cocuy, we can argue that the most abrupt upward changes in the FLH in Los Nevados took place from the Early Otún cold stade to the Late Otún cold stade, and from the Late Otún to the last millennium of the Early Santa Isabel. Such upward shifts were of about half a kilometer in 2,000 years (240 m/millennium) and about half a kilometer in 2,600 years (170 m/millennium), respectively (or approximately 24 to 17 m/century). The most abrupt upward changes in Sierra Nevada del Cocuy occurred in the last millennium of the Early Lagunillas cold stade and during the rapid warming period between the Late Lagunillas and the Bocatoma cold stades. The upward changes reached extraordinary values of about half a kilometer in 500 years (i.e., 1,000 m/millennium) and 650 m in 800 years (i.e., 813 m/millennium), respectively (or approximately 100 to 83 m/century). The velocities of altitudinal change in both study sites are consistent with the 200 to 230 m/°C Equilibrium Line Altitude sensitivity proposed by Sagredo et al. (2014) for the inner tropics. Compared to the maximum upward changes that likely took place over the past ca. 20,000 years in our two areas of interest, the observed (present-day) upward shifts of the FLH have occurred at a rate that significantly surpasses the inferred rates: from 36 to 50 times and from 8.5 to 10 times faster.

7 Conclusions

We propose here a freely accessible online climate data-driven approach, combined with field-based geomorphological mapping, to infer changes in the freezing level height in the upper ranges of the northern Andes, in order to understand how fast climatic changes have occurred in the region. We implemented the methodology in a study site in the Colombian Central cordillera and replicated its steps in a comparative study site in the Eastern cordillera (the Sierra Nevada del Cocuy). Our methodology included the combined signals of the main modes of spatio-temporal variability of SSTs in the Atlantic and Pacific oceans. Specifically, the inferred environmental lapse rates for the main and comparative study sites were informed by reconstructed sea surface temperature anomalies in the tropical Atlantic and in the central to eastern equatorial Pacific, respectively. The air temperatures at sea level for the two study sites were controlled by the same anomalies in these two ocean basins but in the opposite order; i.e., the main study site was influenced by the central to eastern equatorial Pacific, whereas the comparative site in Sierra Nevada was influenced by the tropical Atlantic. Our methodology also included refined assumptions and extrapolations proposed for the areas of interest, based on available, historical near-surface and free air temperature datasets from reanalysis products, General Circulation Model simulations, weather stations, and digital sensors.

The methodology has important sources of uncertainty that need to be explicitly mentioned. The main uncertainties come from the inherent uncertainties of the paleoclimatic reconstructions of SSTs and relative sea level and our assumptions of air-sea interactions and environmental lapse rates. For the analysis of air-sea temperature differences, we restricted the spatial domain of SSTs to a specific area within the tropical eastern Pacific [12.5°S-12.5°N, 170°W-90°W], but ignored its internal spatial variability. Thus, we made no distinction between the grid points of the geographic domain exhibiting SSTs above the minimum threshold required for deep convection, which in the case of the tropical eastern Pacific needs to be explicitly addressed given the marked differences between grid points within and outside the cold tongue. Secondly, we assumed only the mean and standard deviation of the temperature differences between the sea and the air right above the surface, ignoring that such a difference exhibits a distribution for all the seasons. We picked the maximum air-sea temperature difference with the lesser spatial variability (-0.37±0.39 K) based on

present-day conditions observed during the quarter March-April-May. Such a period comprises the month when the maximum extent of ocean surface area with SSTs above the 300 K threshold is observed. Lastly, we assumed the same normal distribution of air-sea temperature differences for the full extent of the reconstruction period.

We argue that our reconstruction of the changes in the FLH could narrow down the coarse resolution of glacier advances suggested for the main study site on the Ruiz-Tolima volcanic massif by previous research efforts. By studying fluctuations in the 0°C isotherm, our data-driven methodology could provide insights into our overall understanding of past climatic changes and present trends in the region of interest, and fill in several spatial gaps in the distribution of chronologic studies in the northern Andes. However, we warn that the method applied here cannot be analytically better than the implementation of cosmic ray exposure dating for chronological constraints of glacier evolution. Our research could also facilitate the analysis of the signals of natural and anthropogenic climate change in the region, and the assessment of their impacts on the integrity of high-altitude environments. We concur with the statement by Rodbell et al. (2009) who argue that all of the Andes north of the Equator require further study. We think that there is an urgent need to include these findings in the assessment of future likely changes in the spatial distribution of high-altitude Andean ecosystems and their integrity in a future warmer world.

8 Data Sources

Kienast et al. (2006) reconstructed SST data, available at the World Data Center for Paleoclimatology and the NOAA Paleoclimatology Program - Paleocean Site Data, can be downloaded at: https://www1.ncdc.noaa.gov/pub/data/paleo/paleocean/by_contributor/kienast2006b/kienast2006b.txt.

Bova et al. (2015) reconstructed SST data, also available at the World Data Center for Paleoclimatology and the NOAA Paleoclimatology Program - Paleocean Site Data, can be downloaded at: http://www1.ncdc.noaa.gov/pub/data/paleo/paleocean/by_contributor/bova2015/bova2015-cdh26-uk37.txt.

Dyez et al. (2016) reconstructed SST data, also available at the World Data Center for Paleoclimatology and the NOAA Paleoclimatology Program - Paleocean Site Data, can be accessed at: http://www1.ncdc.noaa.gov/pub/data/paleo/paleocean/by_contributor/dyez2016/dyez2016-sst-merge.txt.

Lea et al. (2003) reconstructed SST data, also available at the World Data Center for Paleoclimatology and the NOAA Paleoclimatology Program - Paleoclimatology Data, can be accessed at: https://www.ncdc.noaa.gov/paleo-search/study/6310.

Lea et al. (2000, 2002) reconstructed sea level data can be accessed at: ftp://ftp.ncdc.noaa.gov/pub/data/paleo/contributions_by_author/lea2002/lea2002.txt.

Kaplan's SSTa data can be downloaded from the Data Library of the International Research Institute for Climate and Society – IRI at: http://iridl.ldeo.columbia.edu/SOURCES/.KAPLAN/.EXTENDED/.v2/.ssta/.

The ATLAS7 GOSTA climatological fields can be downloaded from the IRI Data Library at: http://iridl.ldeo.columbia.edu/expert/SOURCES/.GOSTA/.atlas7/.climatology/.5deg/.sst/.

The NOAA NCDC ERSST version2 SST data can be downloaded from the IRI Data Library at: http://iridl.ldeo.columbia.edu/SOURCES/.NOAA/.NCDC/.ERSST/.version2/.SST/.

Niño 1+2 SST data were downloaded from the Global Climate Observing System (GCOS) Working Group on Surface Pressure (Rayner et al., 2003): https://www.esrl.noaa.gov/psd/gcos_wgsp/Timeseries/Nino012/.

Niño 3.4 SST data were downloaded from the Equatorial Pacific Sea Surface Temperatures web site of the US National Oceanic and Atmospheric Administration – NOAA: https://www.ncdc.noaa.gov/teleconnections/enso/indicators/sst.php.

LEVITUS94 SST fields can be downloaded from the IRI Data Library at: http://iridl.ldeo.columbia.edu/SOURCES/.LEVITUS94/.MONTHLY/.temp/.

ECHAM4.5 monthly ensemble simulation runs can be downloaded from the IRI Data Library at: http://iridl.ldeo.columbia.edu/SOURCES/.IRI/.FD/.ECHAM4p5/.History/.MONTHLY/.PressureLevel-SF/.ta/.

NOAA NCEP/DOE AMIP-II Reanalysis-2 data can be downloaded from the IRI Data Library at: http://iridl.ldeo.columbia.edu/SOURCES/.NOAA/.NCEP-DOE/.Reanalysis-2/.Monthly/.flx/.c8009/.tmp2m/ and at http://iridl.ldeo.columbia.edu/SOURCES/.NOAA/.NCEP-DOE/.Reanalysis-

2/.Monthly/.pgb/.pgb/.tmpprs/.

NARR data can be downloaded at: http://www.esrl.noaa.gov/psd/data/gridded/data.narr.pressure.html.

ERA-Interim reanalysis data can be downloaded at: http://apps.ecmwf.int/datasets/data/interim-full-daily/?levtype=pl.

The quality-controlled weather stations included: 2615515 Las Brisas (altitude: 4,150 m; instrumental period: 1981-2003), 2125512 Villa Hermosa (2,029 m; 1978-2005), 2612506 El Edén (1,204; 1978-2007), 2615502 Cenicafé (1,310 m; 1950-2007), 2613505 Naranjal (1,381; 1956-2007), 2615509 Santagueda (1,026 m; 1956-2005), 2613507 El Cedral (2,120 m; 1961-2006), 2612524 La Catalina (2,088 m; 1987-2007), 2613506 El Jazmín (1,635 m; 1975-2006), and 2125513 La Trinidad (1,456 m; 1976-2006).

The U23-001 HOBO® data loggers were installed every ~300 m and include: 10667797 Finca Buenavista (1,611 m), 10667798 Claro-Molinos (1,917 m), 10667799 Molinos (2,274 m), 10409123 La Quinta (2,599 m), 10409121 San Antonio (3,084 m), 10409122 La Fonda (3,500 m), 2272886 Salto Cueva (3,790 m), 2272887 Microcentral (3,910 m), 2272888 El Cisne (4,000 m), 2272889 Nariz Diablo (4,260 m), 10047204 Lupinus Valley (4,600 m), and 9950000 Santa Isabel (4,891 m). Hourly records can be downloaded at: http://data.cuahsi.org/.

References

Bakker JGM, Salomons JB (1989) A palaeoecological record of a volcanic soil sequence in the Nevado del Ruiz area, Colombia. Rev Palaeobot Palyno 60: 149-163. https://doi.org/10.1016/0034-6667(89)90074-2

Benn DI, Evans DJA (2010) Glaciers and glaciation. 2nd edition, Routledge, London: Hodder Education. 802 (2010). https://doi.org/10.4324/9780203785010

Bottomley M, Folland CK, Hsiung J (1990) Global Ocean Surface Temperature Atlas. Met. Office.

Bova SC, Herbert T, Rosenthal Y, et al. (2015) Links between eastern equatorial Pacific stratification and atmospheric CO_2 rise during the last deglaciation. Paleoceanography 30:1407-1424. https://doi.org/10.1002/2015PA002816

Bradley RS, Keimig FT, Díaz HF (2004) Projected temperature change along the American cordillera and the planned GCOS network. Geophys Res Lett 31: L16210. https://doi.org/10.1029/2004GL020229

Bradley RS, Keimig FT, Díaz HF, et al. (2009) Recent changes in freezing level heights in the tropics with implications for the deglacierization of high mountain regions. Geophys Res Lett 36: L17701. https://doi.org/10.1029/2009GL037712

Bradley RS, Vuille M, Díaz HF, et al. (2006) Threats to water supplies in the tropical Andes. Science 312 (5781): 1755–1756. https://doi.org/10.1126/science.1128087

Braitmeyer M (2003) The surface energy balance of Santa Isabel Nevado, Colombia. PhD thesis. Dusseldorf University. (In German)

Bromley G, Ruiz D, Restrepo-Moreno SA (2013) Reconstructing Late Quaternary tropical glacier change in the Colombian Andes through surface-exposure dating. Memorias del XIV Congreso Colombiano de Geología, Bogotá, Colombia. ISBN 978-958-57950-0-6.

Bush MB, Colinvaux PA, Weimann MC, et al. (1990) Late Pleistocene temperature depression and vegetation change in Ecuadorian Amazonia. Quaternary Res 34: 330–345. https://doi.org/10.1016/0033-5894(90)90045-M

Clapperton CM (1993) Nature of environmental changes in South America at the Last Glacial Maximum. Palaeogeogr Palaeocl 101: 189–208. https://doi.org/10.1016/0031-0182(93)90012-8

Clark PU, Dyke AS, Shakun JD, et al. (2009). The Last Glacial Maximum. Science 325: 710–714. https://doi.org/10.1126/science.1172873

Cleef AM (1979) The phytogeographical position in the neotropical vascular páramo flora with special reference to the Colombian Cordillera Oriental. Tropical Botany. Academic Press Inc., London. pp 175-184.

Cleef AM, Noldus GW, van der Hammen T (1995) Palynological study of the Middle Pleniglacial in the Otono river - Manizales Enea cross section, (Central Cordillera, Colombia). In: van der Hammen T, dos Santos AG (eds.), Studies on Tropical Andean Ecosystems. (In Spanish)

Dansgaard W, Johnsen SJ, Clausen HB, et al. (1993) Evidence for general instability of past climate from a 250-ka ice-core record. Nature 364: 218-220. https://doi.org/10.1038/364218a0

Dyez KA, Ravelo AC, Mix AC (2016) Evaluating drivers of Pleistocene eastern tropical Pacific sea surface temperature. Paleoceanography 31(8): 1054-1069. https://doi.org/10.1002/2015PA002873

Flórez A (1992a) Remaining glaciers in Colombia: geo-historical approach and current situation. Zenit 3: 35-45. (In Spanish)

Flórez A (1992b) Colombian nevados: glaciers and glaciations. Geographical Analyses 22. Agustin Codazzi Geographical Institute- IGAC, Bogota. (In Spanish)

Francou B, Vuille M, Favier V, et al. (2004) New evidence for an ENSO impact on low-latitude glaciers: Antizana 15, Andes of Ecuador, 0°28'S. J Geophys Res: Atmospheres 109. https://doi.org/10.1029/2003JD004484

Greenland Ice-core Project (GRIP) Members (1993) Climate instability during the last interglacial period recorded in the GRIP ice core. Nature 364: 203-207. https://doi.org/10.1038/364203a0

Harris GN, Bowman KP, Shin DB (2000) Comparison of freezing-level altitudes from the NCEP reanalysis with TRMM precipitation radar brightband data. J Clim 13: 4137-4148. https://doi.org/10.1175/1520-0442(2000)013%3C4137:COFLAF%3E2.0.CO;2

Hastings DA, Dunbar PK (1999) Global land one-kilometer base elevation (GLOBE) digital elevation model, Documentation, Volume 1.0. Key to Geophysical Records Documentation (KGRD) 34. National Oceanic and Atmospheric Administration, National Geophysical Data Center, 325 Broadway, Boulder, Colorado 80303, USA.

Herd DG (1982) Glacial and volcanic geology of the Ruiz-Tolima volcanic complex, Cordillera Central, Colombia. Ingeominas Special Geological Publications, Bogota, Colombia. 8: 1-48. (In Spanish)

Hooghiemstra H (1984) Vegetational and climatic history of the high plain of Bogotá, Colombia: a continuous record of 3.5 million years. Dissertationes Botanicae, Vol. 79.

Hooghiemstra H, van der Hammen T (2004) Quaternary ice-age dynamics in the Colombian Andes: developing an understanding of our legacy. Philos T Roy Soc B 359:173–181. https://doi.org/10.1098/rstb.2003.1420

Institute for Hydrology, Meteorology and Environmental

Studies - IDEAM (2018) Report of the state of Colombian glaciers. Bogota, Colombia. p 36. (In Spanish)]

Jomelli V, Favier V, Vuille M, et al. (2014) A major advance of tropical Andean glaciers during the Antarctic cold reversal. Nature 513: 224-228. https://doi.org/10.1038/nature13546

Jouzel J, Lorius C, Petit JR, et al. (1987) Vostok ice core: a continuous isotope temperature record over the last climatic cycle (160,000 years). Nature 329 (6138): 403-408. https://doi.org/10.1038/329403a0

Kanamitsu M, Ebisuzaki W, Woollen J, et al. (2002) NCEP-DOE AMIP-II Reanalysis (R-2). Bull Amer Meteor Soc 83: 1631-1643.

Kaplan A, Cane M, Kushnir Y, et al. (1998) Analyses of global sea surface temperature 1856-1991. J Geophys Res 103(18): 567-589. https://doi.org/10.1029/97JC01736

Kaser G (2001) Glacier-climate interaction at low latitudes. J Glaciol 47: 195–204. https://doi.org/10.3189/172756501781832296

Kaser G, Juen I, Georges C, et al. (2003) The impact of glaciers on the runoff and the reconstruction of mass balance history from hydrological data in the tropical Cordillera Blanca, Peru. J Hydrol 282: 130-144. https://doi.org/10.1016/S0022-1694(03)00259-2

Kaser G, Osmaston HA (2002) Tropical glaciers. Cambridge University Press, New York. p 209.

Kaser G, Georges Ch (1999) On the mass balance of low latitude glaciers with particular consideration of the Peruvian Cordillera Blanca. Geogr Ann A 81(4): 643-651. https://doi.org/10.1111/1468-0459.00092

Kaufman D, McKay N, Routson C, et al. (2020) Holocene global mean surface temperature, a multi-method reconstruction approach. Sci Data 7: 201. https://doi.org/10.1038/s41597-020-0530-7

Kienast M, Kienast SS, Calvert SE, et al. (2006) Eastern Pacific cooling and Atlantic overturning circulation during the last deglaciation. Nature 443(7113): 846-849. https://doi.org/10.1038/nature05222

Klein AG, Seltzer GO, Isacks BL (1999) Modern and last Local Glacial Maximum snowlines in the central Andes of Peru, Bolivia and Northern Chile. Quaternary Sci Rev 18: 65-86. https://doi.org/10.1016/S0277-3791(98)00095-X

Kuhry P, Salomons JB, Riezebos PA, et al. (1983) Palaeoecology of the last 6,000 years in the surroundings of the Lagoon of the Otun-El Bosque. In: van der Hammen T, Pérez PA, Pinto P (eds.), Studies on Tropical Andean Ecosystems. Volume 1. Cramer (Borntraeger), Berlin/Stuttgart, Germany. pp 227-261. (In Spanish)

Lea DW, Pak DK, Spero HJ (2000) Climate impact of late Quaternary equatorial Pacific sea surface temperature variations. Science 289:1719-1724. https://doi.org/10.1126/science.289.5485.1719

Lea DW, Martin PA, Pak DK, et al. (2002) Reconstructing a 350 kyr history of sea level using planktonic Mg/Ca and oxygen isotopic records from a Cocos Ridge core. Quat Sci Rev 21(1-3): 283-293. https://doi.org/10.1016/S0277-3791(01)00081-6

Lea DW, Pak DK, Peterson LC, et al. (2003) Synchroneity of tropical and high-latitude Atlantic temperatures over the Last Glacial Termination. Science 301: 1361-1364. https://doi.org/10.1126/science.1088470

Levitus S, Boyer TP (1994) World Ocean Atlas 1994. Volume 4: Temperature, Number 4.

López-Arenas CD, Ramírez-Cadena J (ed.) (2010) Glaciers, Snow and Ice of Latin America - Climate Change and Hazards. Collection Glaciers, Nevados and Environment, Colombian Institute of Geology and Mining - INGEOMINAS, Ministry of Mines and Energy, Republic of Colombia. p 343. (In Spanish)

Marcott SA, Shakun JD, Clark PU, et al. (2013) A reconstruction of regional and global temperature for the past 11,300 years. Science 339: 1198-1201. https://doi.org/10.1126/science.1228026

Mölg N, Ceballos JL, Huggel Ch, et al. (2017) Ten years of monthly mass balance of Conejeras glacier, Colombia, and

their evaluation using different interpolation methods. Geogr Ann A 99(2): 155-176. https://doi.org/10.1080/04353676.2017.1297678

Palacios D, Stokes Ch.R, Phillips FM, et al. (2020) The deglaciation of the Americas during the Last Glacial Termination. Earth-Sci Rev 203: 103113. https://doi.org/10.1016/j.earscirev.2020.103113

Parker DE, Jones PD, Folland CK, et al. (1994) Interdecadal changes of surface temperature since the late nineteenth century. J Geophys Res 99(14): 373-399. https://doi.org/10.1029/94JD00548

Pepin N, Bradley RS, Diaz HF, et al. (2015) Elevation-dependent warming in mountain regions of the world. Nat Clim Chang 5: 424-430. https://doi.org/10.1038/nclimate2563

Petit JR, Mourner L, Jouzel J, et al. (1990) Palaeoclimatological and chronological implications of the Vostok core dust record. Nature 343: 56-58. https://doi.org/10.1038/343056a0

Qixiang W, Wang M, Fan X (2018) Seasonal patterns of warming amplification of high-elevation stations across the globe. Int J Climatol 38: 3466-3473. https://doi.org/10.1002/joc.5509

Rabatel A, Francou B, Soruco A, et al. (2013) Current state of glaciers in the tropical Andes: a multi-century perspective on glacier evolution and climate change. Cryosphere 7: 81-102. https://doi.org/10.5194/tc-7-81-2013

Ramanathan V, Collins W (1991) Thermodynamic regulation of ocean warming by cirrus clouds deduced from observations of the 1987 El Niño. Nature 351: 27-32. https://doi.org/10.1038/351027a0

Rayner NA, Parker DE, Horton EB, et al. (2003) Global analyses of sea surface temperature, sea ice, and night marine air temperature since the late nineteenth century. J Geophys Res 108 (D14): 4407. https://doi.org/10.1029/2002JD002670

Reynolds RW, Smith TM (1994) Improved global sea surface temperature analysis using optimum interpolation. J Climate 7: 929-948. https://doi.org/10.1175/1520-0442(1994)007%3C0929:IGSSTA%3E2.0.CO;2

Rodbell DT, Smith JA, Mark BG (2009) Glaciation in the Andes during the Lateglacial and Holocene. Quaternary Sci Rev 28(21-22): 2165-2212. ISSN 0277-3791. https://doi.org/10.1016/j.quascirev.2009.03.012

Roeckner E, Arpe K, Bengtsson L, et al. (1996) The atmospheric general circulation model ECHAM4: model description and simulation of present-day climate. Max-Planck-Institut fur Meteorologie Rep. 218, Hamburg, Germany. p 90.

Ruiz D, Arroyave MP, Gutiérrez ME, et al. (2011) Increased climatic stress on high-Andean ecosystems in the Cordillera Central of Colombia. pp. 182-191. In: Herzog SK, Martínez R, Jørgensen PM, Tiessen H (eds.), Climate Change and Biodiversity in the Tropical Andes. MacArthur Foundation, Inter-American Institute of Global Change Research (IAI) and Scientific Committee on Problems of the Environment (SCOPE), São José dos Campos and Paris. p 348. ISBN: 978-85-99875-05-6.

Ruiz-Carrascal D (2016) Poleka Kasue Mountain Observatory, Los Nevados Natural Park, Colombia. Joint Issue Mountain Views/Mountain Meridian, Consortium for Integrated Climate Research in Western Mountains (CIRMOUNT) and Mountain Research Initiative (MRI), Vol 10, Number 2, December 2016. pp 17-20.

Sagredo E, Lowell T (2012) Climatology of Andean glaciers: a framework to understand glacier response to climate change. Global Planet Change 86-87: 101-109. https://doi.org/10.1016/j.gloplacha.2012.02.010

Sagredo E, Rupper S, Lowell T (2014) Sensitivities of the equilibrium line altitude to temperature and precipitation changes along the Andes. Quaternary Res 81(2): 355-366. https://doi.org/10.1016/j.yqres.2014.01.008

Salomons JB (1986) Paleoecology of volcanic soils in the Colombian Central Cordillera (Parque Nacional Natural de Los Nevados). Ph.D. thesis. University of Amsterdam,

Netherlands. The Quaternary of Colombia. p 13.

Schauwecker S, Rohrer M, Acuna D, et al. (2014) Climate trends and glacier retreat in the Cordillera Blanca, Peru, revisited. Glob Planet Chang 119: 85-97.
https://doi.org/10.1016/j.gloplacha.2014.05.005

Schauwecker S, Rohrer M, Huggel C, et al. (2017) The freezing level in the tropical Andes, Peru: an indicator for present and future glacier extents. Geophys Res Atmospheres 122: 5172-5189. https://doi.org/10.1002/2016JD025943

Shakun JD, Clark PU, He F, et al. (2012) Global warming preceded by increasing carbon dioxide concentrations during the last deglaciation. Nature 484: 49-54.
https://doi.org/10.1038/nature10915

Smith TM, Reynolds RW (2004) Improved extended reconstruction of SST [1854-1997]. J Climate 17: 2466-2477.
https://doi.org/10.1175/1520-0442(2004)017%3C2466:IEROS%3E2.0.CO;2

Thompson LG, Davis M, Mosley-Thompson E, et al. (1988) Pre-Incan agricultural activity recorded in dust layers in two tropical ice cores. Nature 336: 763-765.
https://doi.org/10.1038/336763a0

Thompson LG, Davis ME, Mosley-Thompson E, et al. (1998) A 25,000-year tropical climate history from Bolivian ice cores. Science 282: 1858-1864.
https://doi.org/10.1126/science.282.5395.1858

Thompson LG, Mosley-Thompson E, Morales-Arnao BM (1984) Major El Niño-Southern Oscillation events recorded in stratigraphy of the tropical Quelccaya ice cap. Science 226: 50-52. https://doi.org/10.1126/science.226.4670.50

Thompson LG, Mosley-Thompson E, Bolzan JF, et al. (1985) A 1,500 year record of tropical precipitation recorded in ice cores from the Quelccaya ice cap, Peru. Science 229: 971-973.
https://doi.org/10.1126/science.229.4717.971

Thompson LG, Mosley-Thompson E, Dansgaard W, et al. (1986) The 'Little Ice Age' as recorded in the stratigraphy of the tropical Quelccaya ice cap. Science 234: 361-364.
https://doi.org/10.1126/science.234.4774.361

Thompson LG, Mosley-Thompson E, Davis ME, et al. (1995) Late Glacial Stage and Holocene tropical ice core records from Huascarán, Peru. Science 269: 46-50.
https://doi.org/10.1126/science.269.5220.46

Thompson LG, Mosley-Thompson E, Henderson KA (2000) Ice-core palaeoclimate records in tropical South America since the Last Glacial Maximum. J Quaternary Sci 15: 377-394.
https://doi.org/10.1002/1099-1417(200005)15:4%3C377::AID-JQS542%3E3.0.CO;2-L

Thouret JC, van der Hammen T, Salomons B (1996) Palaeoenvironmental changes and glacial stades of the last 50,000 years in the Cordillera Central, Colombia. Quaternary Res 46: 1-18. https://doi.org/10.1006/qres.1996.0039

Thouret JC, van der Hammen T, Salomons B, et al. (1997) Late Quaternary glacial stages in the Cordillera Central, Colombia, based on glacial geomorphology, tephra-soil stratigraphy, palynology, and radiocarbon dating. J Quaternary Sci 12(5): 347-369.
https://doi.org/10.1002/(SICI)1099-1417(199709/10)12:5%3C347::AID-JQS319%3E3.0.CO;2-%23

Torres V, Hooghiemstra H, Lourens L, et al. (2013) Astronomical tuning of long pollen records reveals the dynamic history of montane biomes and lake levels in the tropical high Andes during the Quaternary. Quaternary Sci Rev 63: 59-72.
https://doi.org/10.1016/j.quascirev.2012.11.004

van der Hammen T (1974) The Pleistocene changes of vegetation and climate in tropical South America. J Biogeogr 1: 3-26. https://doi.org/10.2307/3038066

van der Hammen T, Barelds J, De Jong H, et al. (1980/1981) Glacial sequence and environmental history in the Sierra Nevada del Cocuy (Colombia). Palaeogeogr Palaeocl 32: 247-340. https://doi.org/10.1016/0031-0182(80)90043-7

van der Hammen T (1989) La Cordillera Central Colombiana – Transecto Parque de Los Nevados. Berlín: Stuttgart.

Velasquez FH (1998) The Little Ice Age in the Ruiz and Santa Isabel Nevados. Undergraduate thesis. Medellin: National University of Colombia, Department of Geological Engineering. (In Spanish)

Vuille M, Bradley RS (2000) Mean annual temperature trends and their vertical structure in the tropical Andes. Geophys Res Lett 27: 3885-3888. https://doi.org/10.1029/2000GL011871

Vuille M, Carey M, Huggel Ch, et al. (2018) Rapid decline of snow and ice in the tropical Andes – Impacts, uncertainties and challenges ahead. Earth-Sci Rev 176: 195–213.
https://doi.org/10.1016/j.earscirev.2017.09.019

Vuille M, Francou B, Wagnon P, et al. (2008) Climate change and tropical Andean glaciers - past, present and future. Earth Sci Rev 89: 79-96.
https://doi.org/10.1016/j.earscirev.2008.04.002

Vuille M, Franquist E, Garreaud R, et al. (2015) Impact of the global warming hiatus on Andean temperature. J Geophys Res 120(9): 3745-3757.
https://doi.org/10.1002/2015JD023126

Waelbroeck C, Labeyrie L, Michel E, et al. (2002) Sea-level and deep water temperature changes derived from benthic *foraminifera* isotopic records. Quaternary Sci Rev 21(1-3): 295-305. https://doi.org/10.1016/S0277-3791(01)00101-9

Wang Q, Fan X, Wang M (2016) Evidence of high-elevation amplification versus Arctic amplification. Sci Rep 6: 19219.
https://doi.org/10.1038/srep19219

Williams Jr. RS, Ferrigno JG (1999) Satellite image atlas of glaciers of the world. U.S. Geological Survey Professional Paper 1386-I. United States Government Printing Office, Washington D.C..